EVOLUTION OF REAL MUNICIPAL WASTEWATER TREATMENT IN PHOTOBIOREACTORS AND MICROALGAE-BACTERIA CONSORTIA USING REAL-TIME PARAMETERS

Foladori P.[a,*], Petrini S.[a], Andreottola G. [a]

[a] Department of Civil, Environmental and Mechanical Engineering, University of Trento, via Mesiano 77, 38123 Trento, Italy.
* Corresponding author. E-mail: paola.foladori@unitn.it

Abstract

In the treatment of real municipal wastewater with photo-sequencing batch reactors (PSBR), operating strategies able to achieve high levels of pollutant removal, but reduce the hydraulic retention time (HRT), are imperative for making microalgae-bacteria consortia more competitive than conventional activated sludge systems. In regard to real-time monitoring, on-line probes like Dissolved Oxygen (DO), pH and oxidation-reduction potential (ORP) are cheap and reliable, but their exploitation has been largely overlooked in PSBRs. This paper proposes the use of DO, pH and ORP profiles to reveal the evolution of wastewater treatment in a PSBR treating real municipal wastewater with a mixed consortium of microalgae and bacteria. The PSBR ensured removal efficiency of 87±5% for COD and 98±2% for TKN without external aeration; indeed, photosynthesis was the only driver of the oxygen production. Considering the combined effects of photosynthetic oxygenation and microbial oxygen consumption, some practical information was gathered to understand the complex profiles of the on-line parameters. During dark and light phases, Zero-DO values, DO and pH raises, and their relative peaks were discussed to evaluate correctly

the conclusion of the wastewater treatment and therefore to adjust the duration of the PSBR cycle. In particular: (1) two simultaneous "characteristic points", "Ammonia valley" (pH profile) and "DO breakpoint" (DO profile), detected univocally the complete ammonium removal; (2) the absolute peaks of DO, pH and ORP at maximum irradiance revealed that wastewater treatment was complete and the cycle could be concluded. In this way, these characteristic points were exploited for the optimization of the PSBR cycle, which was concluded after 15-26 h, reducing the HRT by more than 45%.

Keywords. Microalgae; Photobioreactor; On-line monitoring; Wastewater treatment; Nitrification.

1. INTRODUCTION

Microalgal-based wastewater treatments have been studied since the early 1950s [1]. However, in recent years, they have received increasing attention due to the sustainability of engineered photobioreactors that are moving towards small footprint and energy saving. The growing problem of global warming, the increasing energy consumption in the water sector, and the high costs of excess sludge disposal entail a paradigm shift in the configurations of conventional wastewater treatment plants (WWTPs) to become more environmentally and economically sustainable. In this regard, a particularly attractive alternative may be the use of microalgae-bacteria consortia as an engineered system, where symbiotic relations between microalgae and bacteria may be advantageously exploited for wastewater treatment [2,3,4,5,6]. Most of the recent literature focuses on the use of pure microalgae strains to treat synthetic wastewater (or filtered wastewater) excluding bacteria inocula and

58 microorganisms naturally present in real wastewater. Therefore, the reproducibility of
59 real operational conditions of WWTPs is limited because the development of complex
60 and heterogeneous consortia of microalgae, cyanobacteria and aerobic/anaerobic
61 microorganisms, is hindered. Although microalgae and natural algal blooms have been
62 tested in combination with enriched bacterial strains [7,8] or activated sludge [5,9,10],
63 the scientific literature on the treatment of real wastewater with microalgal-bacterial
64 consortia is still extremely scant.
65 Suspended-biomass reactors operating at lab scale as photo-sequencing batch reactors
66 (PSBR) are among the configurations most used for the implementation of microalgal
67 consortia [11]. PSBRs offer the advantages of batch feed and sequencing phases that are
68 operations easy to implement and control.
69 Knowledge about pollutant removal in PSBRs with microalgal-bacterial consortia is
70 still in its infancy. However, preliminary results appear promising. García et al. [12]
71 observed in a photobioreactor with hydraulic retention time (HRT) of 2 days, an organic
72 matter removal of 89±2%, similar to that typically achieved in conventional activated
73 sludge systems and in conventional high rate algal ponds treating domestic wastewater.
74 Regarding total nitrogen and ammonium removal, microalgal-based systems may be
75 inefficient (e.g. slow nitrogen assimilation, low efficiency of NH_4^+ nitrification)
76 requiring very long HRTs in the range of 2-5 days [13,14]. In contrast, HRTs up to 1
77 day are enough to obtain nitrogen removal efficiencies of 60-80% in conventional
78 nitrification-denitrification activated sludge systems. Therefore, the design of operating
79 strategies able to achieve high levels of nitrogen removal with reasonable HRTs is
80 essential to make microalgal-bacterial consortia more competitive than activated sludge
81 systems, especially for PSBRs.
82 PSBRs monitoring is usually based on chemical analyses. Although chemical analyses
83 are essential for evaluating effluent quality and pollutants removed loads, they are

84 expensive, time-consuming and cannot be exploited in real-time because they are
85 available with a certain delay. For real-time monitoring, on-line analyzers of direct
86 chemical parameters (such as ammonium, nitrate+nitrite, phosphate, etc.) could be
87 applied, but they require a certain level of maintenance - in some cases, frequent
88 calibrations - and they are not always accessible at reasonable costs. Conversely, probes
89 that measure indirect parameters such as Dissolved Oxygen (DO), pH and oxidation-
90 reduction potential (ORP), are cheap, robust, reliable and user-friendly [15,16].
91 The importance of real-time monitoring based on DO, pH and ORP profiles has already
92 been demonstrated in activated sludge systems such as sequencing batch reactors
93 (SBRs) and alternating oxic-anoxic activated sludge [15,17,18]. In these studies,
94 variations along profiles have made it possible to detect "characteristic points" useful
95 for understanding the ongoing biological processes [19]. More precisely, a characteristic
96 point is a key indicator of the activated sludge process, denoted by a sharp change along
97 a parameter profile. Usually, this variation coincides with the depletion of a compound
98 or the transition from one process to another. For example, the end of nitrification in
99 activated sludge SBRs can be identified by a point of minimum in the pH profile called
100 "Ammonia Valley" and a flex in the DO curve called "DO breakpoint" that occurs
101 simultaneously [20,21]. Similarly, the end of the denitrification process corresponds to
102 the "nitrate knee", a flex in the ORP profile [20,21]. The presence of a characteristic
103 point may suggest that the treatment process is complete and therefore that the treatment
104 phase can be concluded [17,18,22], while the absence suggests that the cycle needs to
105 be prolonged to guarantee the required removal performance. The variation of online
106 indicator such as pH, ORP and DO were demonstrated closely related with the nutrient
107 removal performance, and this permits to establish the real time control of bioprocesses
108 [23].
109 In regard to photobioreactors, nutrient removal is dependent on a number of parameters,

including DO concentration and pH. Although DO and pH monitoring occurs with a certain frequency in PSBRs [3,7,24,25], the data have not yet been used as means to control or manipulate the process. Indeed, these key parameters appear to have been largely overlooked in PSBRs [13].

Considering the necessity of reducing HRTs of PSBRs, and thus footprint and energy consumption, the possibility to adopt on-line DO/pH/ORP sensors to control and optimize the process, appears very interesting.

This paper explores real time monitoring of DO, pH and ORP in a PSBR treating real municipal wastewater with a mixed consortium of microalgae and bacteria. The objective is to find some characteristic points that may help understand how the treatment process evolves over time.

Microalgae-based processes are affected by natural light. Since photosynthesis produces oxygen and induces pH variations, the evolution of DO, pH and ORP profiles may differ significantly from that observed in activated sludge processes, for which a wide literature exists. In this case, the profiles induced by photosynthetic microorganisms overlap with the profiles produced by bacterial processes. This results in complex 24-h profiles more difficult to understand.

To our knowledge, this is the first time that DO, pH and ORP profiles have been investigated in depth in a PSBR treating real wastewater with a mixed microalgal-bacterial consortium. This paper provides some suggestions on how to understand these profiles in detail.

2. MATERIALS AND METHODS

2.1. Influent wastewater

Influent pre-settled wastewater was collected from the Trento Nord municipal WWTP

(Italy), which treats a population equivalent (PE) around 100,000 PE. Before the feeding in the PSBR, no filtration of the wastewater was performed. In this way, solids and microorganisms naturally present in the pre-settled wastewater were fed into the reactor.

2.2. Photo-sequencing batch reactor and microalgae-bacteria consortium

The PSBR consists of a cylindrical bench-scale reactor made of Pyrex glass (0.29 m high and 0.13 m wide) with a working volume of 2 L, not sealed from atmosphere (Figure 1A). The system was operated with pumps, a lamp and a mixer controlled by timers. Peristaltic pumps (Kronos Seko, Italy) were used to pump the influent and discharge the effluent. The volume of influent wastewater fed into the PSBR every cycle was 0.7 L.

Sunlight entered the laboratory but the reactor was never directly exposed. Consequently, light was also supplied by a cool-white lamp (8 led x 0.5 W; Orion, Italy) arranged on one side of the reactor. Since daylight may vary in intensity and time, the artificial light was used to ensure a photoperiod of 16 h. In this way, a better understanding of on-line profiles was possible because a certain amount of irradiance was guaranteed throughout the light period.

During the reaction phase, the biomass was mixed by a magnetic stirrer set at about 200 rpm to avoid excessive turbulence and reoxygenation from air. To be noted is that absolutely no external aeration was provided. Temperature of mixed liquor was 22.2°C on average. Biomass that occasionally stuck to the reactor walls, was detached in order to allow light penetration into the reactor.

A consortium of microalgae and bacteria was acclimatized for more than one year in the PSBR. Microscopic observations showed the presence of *Chlorella*, *Diatoms* and filamentous cyanobacteria embedded in dense flocs together with a large amount of

heterotrophic bacteria (Figure 1B). This experimentation was carried out on the acclimatized biomass, from November 2016 to March 2017. Total suspended solids (TSS) in the PSBR were maintained at a concentration of approximately 1.3 g TSS/L. This biomass concentration was identified as optimal for fully exploiting volumetric kinetics and light diffusion (data not shown).

< insert Figure 1 here >

2.3. Typical cycle in the PSBR

The PSBR cycle consisted of four phases with a total duration of 48 h: (1) Feed, with a duration of 0.08 h; (2) React, 47.5 h; (3) Settlement, 0.5 h; (4) Draw, 0.08 h. The React phase comprised two photoperiods of 16 h light/8 h dark. The sequence of light periods (LP1, LP2) and dark periods (DP1, DP2) is shown in Figure 2. The cycle started at 8.00 a.m. with the Feed phase. Then, the first light phase (LP1) began immediately after the feeding. The sequence of light and dark resulted in an alternation of periods with high and low DO. As shown in Figure 2, light periods (LPs) affected microalgal photosynthesis, stimulating oxygen production and thus favouring aerobic conditions. Instead, during dark periods (DPs), oxygen was consumed by both bacteria and microalgal respiration, and therefore anoxic conditions occurred.

Due to the good settleability of the biomass (Figure 1C), only a period of 0.5 h was assigned to the Settlement phase.

< insert Figure 2 here >

2.4 Analytical methods

The following chemical parameters were analyzed in influent and effluent wastewater according to Standard Methods [26]: total COD, soluble COD (sCOD), TSS, TKN, NH_4^+-N, NO_2^--N, NO_3^--N and PO_4^{3-}-P. The parameter sCOD was measured after

filtration of the sample on 0.45-μm-membrane. TSS were measured in the mixed liquor, according to APHA [26], to determine the biomass concentration in the PSBR.

DO, pH, ORP and temperature were continuously recorded (every 10 min). DO and temperature were measured with an OXI340i meter coupled with the sensor CellOx®325 and with a Multi3410 meter equipped with the sensor FDO®925 (all from WTW, Germany). The parameters pH and ORP were measured with pH3310 meters coupled with the electrodes Sentix®41 and Sentix®ORP, respectively (all from WTW, Germany).

Light intensity (irradiance, IRR) was measured as photosynthetically active radiation (PAR) using a SQ-520 quantum sensor (Apogee Instruments, USA) placed inside the reactor, near the top of the liquid surface. Artificial light provided an average light intensity of 25±5 μmol quanta·m^{-2}·s^{-2}.

Microscopic observations were performed using a Nikon Optiphot EFD-3 Microscope (Nikon, Japan) to characterize the morphology of the microalgal-bacterial consortium.

2.5 Track studies

Track studies were performed in the PSBR to measure the dynamics of the N-forms during a typical cycle. Samples were collected every hour, then filtered and analysed for NH_4^+, NO_2^- and NO_3^-. The volumetric removal/production rate of nitrogen compounds (mg N L^{-1} h^{-1}) was estimated considering the slope of the straight line that interpolates the experimental concentrations over time. The specific removal/production rate of nitrogen compounds (mg N g TSS^{-1} h^{-1}) was obtained by dividing the volumetric rate by the TSS concentration in the mixed liquor.

3. RESULTS AND DISCUSSION

3.1. PSBR ensures removal efficiency of COD > 85% and TKN > 95% without external aeration

The main characteristics of influent and effluent wastewater together with the removal efficiency are shown in Table 1. The average concentrations of COD, sCOD, TSS, N and P forms in the influent wastewater match typical values expected in pre-settled wastewater [27]. Although real wastewater presented large fluctuations of influent concentrations (Figure 3), high and stable removal efficiency were observed in the PSBR for COD (87±5%, Figure 3A), producing average effluent concentrations of 34±9 mg COD/L and 25±9 mg sCOD/L (Table 1). These results are comparable to those observed in the microalgal treatment of secondary domestic wastewater in outdoors pilot raceways which showed COD removal efficiency in the range 80-90% [28] permitting to respect the discharge limits according to Directive 98/15/CEE.

The effluent TSS concentration was very low (7.4±6.2 mg TSS/L on average), due to the good settleability of the biomass developed in the PSBR which formed dense aggregates of microalgae, bacteria and inerts which entered the system with the real wastewater. This behavior differed significantly from that reported by other studies, where the uses of pure *Chlorella* or other pure strains have often been associated with difficult sedimentation and separation problems [2,29,30]. By contrast, the development of mixed microalgal and bacteria consortia can ensure a significant improvement in settleability [4,11]; hence, they are currently gaining increasing attention in wastewater treatment.

With regard to nitrogen forms, average TKN removal efficiency was 98±2% (Figure 3B). As a result of a stable nitrification in the system, effluent ammonium was 0.6±1.2 mg NH_4^+-N/L, effluent nitrites were negligible, while nitrates were 19.0±7.4 mg NO_3^--N/L. These results are in agreement with the observation of Zhang et al. [31] in algal-bacterial granules in a photobioreactor treating synthetic domestic wastewater. In this

240 study the ammonia removal efficiencies was 97-99%, with negligible values of nitrites
241 and accumulation of nitrates [31].
242 In the microalgal treatment of secondary wastewater, the influence of pH 7-9 on
243 nitrification was negligible and ammonium was rapidly oxidized by nitrification, which
244 prevented N-NH_4^+ stripping [28].
245 The mass balance of total nitrogen indicated that 68±10% was removed by synthesis
246 and spontaneous denitrification. Anoxic conditions favorable for denitrification
247 occurred in various instances: (i) during the dark phases of the PSBR cycle, when DO
248 drop to zero because not supplied by photosynthesis; (ii) during the light phases, when
249 oxygen demand surpassed photosynthetic oxygenation, within the dense clusters of
250 microalgae, bacteria and abiotic solids. For a comparison, Zhang et al. [31] observed
251 TN removal efficiency from 59.8% to 70.5% after the formation of mature granules in a
252 photobioreactor.
253 *< insert Table 1 here >*
254 *< insert Figure 3 here >*
255
256 The detailed monitoring of a typical cycle (48 hours) is shown in Figure 4 where the
257 variations of NH_4^+-N, NO_3^--N and sCOD are indicated over time. The profiles DO and
258 pH were clearly correlated with both light and nutrient removal performance. DO
259 dropped to zero immediately after feeding and remained very low during LP1 and DP1
260 periods, while pH eventually reached a valley due to the nitrification process.
261 The concentration in the influent wastewater was 234 mg COD/L and 78 mg sCOD/L
262 and it decreased during the LP1 period due to the aerobic oxidation, leading to a
263 mimimum sCOD of 21 mg/L.
264 At the beginning of the subsequent LP2 period, pH and DO increased rapidly and
265 sharply as a result of the absence of ammonium and the presence of light which

266 favoured photosynthesis. Surprising, the profile of sCOD correlates with irradiance. A
267 significant release of sCOD was observed in coincidence with the peaks of DO and pH.
268 This behavior is not clear and further investigation is required. The sCOD increase may
269 be the results of the release of Soluble Algal Products but the mechanisms of their
270 formation and their effects are still not clear. At the end of the cycle, the sCOD
271 stabilized, resulting in an effluent COD concentration of 21 mg/L.
272 Since no external aeration was provided, photosynthetic activity was the only driving
273 force to produce the oxygen necessary for COD oxidation and TKN nitrification. Hence,
274 the consortium of cyanobacteria, microalgae and heterotrophic/nitrifying bacteria
275 resulted in a symbiotic system able to ensure a self-sustained treatment process with
276 high removal efficiency of COD and TKN. Similar observations were highlighted by
277 García et al. [12] treating domestic wastewater in a novel anoxic-aerobic
278 photobioreactor.
279 *< insert Figure 4 here >*
280
281 **3.2. The light source affects the shape of the DO profile : sunlight *vs.* artificial light**
282 DO and Irradiance were monitored throughout some typical PSBR cycles. To study the
283 effect of the light source on photosynthetic activity, and thus on DO profile, the feeding
284 phase was skipped. In this way, the influence of oxygen consumed by bacteria to
285 oxidize readily biodegradable substrates was excluded. Without feeding, only
286 endogenous respiration of the biomass occurred. Therefore, the changes of DO in the
287 reactor were mainly associated with light variations, and thus photosynthetic
288 oxygenation, because biomass respiration consumed approximately a small amount of
289 oxygen over time.
290 The effect of sunlight and artificial light on photosynthetic activity was examined in
291 detail. Three different cases were considered. Figure 5 shows the effect of sunlight (5A),

292 artificial light (5B) and both (5C) on DO profile.
293 In the case of sunlight (Figure 5A), the daily variations of irradiance shape a steep and
294 narrow curve with a peak around midday. This produces a perfectly overlapped DO
295 profile with a coinciding peak. Also, Posadas et al. [28], treating primary domestic
296 wastewater in outdoor raceways, showed that DO variations were well correlated with
297 the sunlight, regardless of the raceway configuration and operational conditions.
298 Instead, because artificial light (Figure 5B) produces a constant irradiance, it generates a
299 step-function profile that reflects the adopted photoperiod (lamp on from 08.00 to
300 midnight). As in the case of sunlight, the DO profile follows that of irradiance. Figure
301 5B shows that DO initially increases and then remains approximately constant until the
302 end of the light period. On reaching the saturation level, DO changes smoothly because
303 of temperature (data not shown). As soon as the lamp is turned off, without
304 photosynthetic oxygenation, DO decreases as a result of endogenous respiration.
305 The profile of irradiance produced by sunlight was completely different from that
306 produced by artificial light. Consequently, DO profiles with different shapes were
307 generated by different rates of photosynthesis in the PSBR.
308 In the third case, the combination of sunlight and artificial light (Figure 5C) produces an
309 irradiance profile comparable to the superposition of each individual case. As a
310 consequence, the DO profile is the combination of the single effects previously
311 observed: (i) maximum DO values at midday when solar irradiance is maximum; (ii)
312 relatively high DO values during the whole light-phase supported by artificial light; (iii)
313 gradual DO decrease during the dark when the light is off. As shown in figure 5C, DO
314 values are higher than those obtained with a single light source, in some cases reaching
315 oversaturation level.
316 These simple observations yielded better understanding of the complex DO profiles
317 generated in the PSBR throughout the experimentation, feeding influent real wastewater

318 in the presence of sunlight and artificial light. A detailed description of the observed DO
319 profiles is provided in section 3.3.
320 *< insert Figure 5 here >*
321
322 **3.3. The profiles of DO, pH and ORP reveal the evolution of wastewater treatment**
323 The profiles of irradiance, DO, pH and ORP during three typical cycles in the PSBR,
324 fed with real wastewater, are shown in Figure 6. All the profiles were clearly affected
325 by the alternation of light and dark periods during the cycle and, in particular, by
326 sunlight during the first part of the light periods. As shown in figure 6A, maximum
327 irradiance took place around midday.
328 During a typical cycle very strong variations of parameters occurred:
329 (i) DO varied greatly from zero to oversaturation (Figure 6B). As in the case presented
330 in Figure 5C, the DO profile followed that of irradiance. However, feeding
331 wastewater resulted in a long period at DO zero over the first part of the cycle.
332 Hence, much larger DO variations were observed;
333 (ii) pH ranged from 7.5 to 9.0 (Figure 6C);
334 (iii) ORP changed from negative values immediately after feeding (around -200 mV), to
335 positive values at the end of the light periods (around +200 mV). This change
336 indicates the transition from an initial reducing environment (negative ORP values)
337 to an oxidizing environment (positive values) (Figure 6D). It is well known that the
338 ORP measurement is not a true thermodynamic parameter and that the absolute
339 ORP value does not furnish any process significance, it being a mere indicator of
340 the oxidative-reductive state of the system.
341 *< insert Figure 6 here >*
342
343 On simultaneous consideration of the profiles of irradiance, DO, pH and ORP (Figure

6A, B, C, D, respectively), it is possible to identify a sequence of significant phases for each cycle:

1) "Zero-DO+light" phase (progressive time = 0-16 h): this usually coincides with the first light period (LP1) and is characterized by DO values close to zero (Figure 6B). Immediately after the feeding phase, the system requires a huge amount of oxygen to oxidize the biodegradable substrates and ammonium of the influent wastewater. Since this phase is identified during the LP1, light is available (figure 6A) and thus photosynthesis occurs. Although oxygen is continuously provided in the system, it is not enough to satisfy the requirement of the biomass. Therefore, DO is zero (Figure 6A) because oxygen is immediately consumed by bacteria to oxidize biodegradable COD and NH_4^+. Other studies confirmed that nitrifiers were active in removing ammonium even if the oxygen concentration was close to 0 mg/L [32].
In some cycles, a very short DO peak may appear in this phase, in particular around midday when solar irradiation is maximum. As explained in section 3.2, photosynthesis is affected by available light, and hence a peak of the irradiance could result in a higher oxygen production that may momentarily surpass the biological demand. As a consequence of enhanced photosynthetic activity, also a pH peak may be noted (Figure 6C). Photosynthesis induces pH increase because of HCO_3^- uptake (see section 3.3.2). Figure 6C shows that after the maximum irradiance, pH decreased until the end of this phase. Therefore, there was another process that counterbalanced the photosynthesis effect on pH. Since wastewater contains ammonia, the pH decrease was induced by nitrifying bacteria (see section 3.3.1).
This phase presents conditions with apparently no oxygen, but it must not be confused with an anoxic phase where oxygen is not available. In fact, even if DO is zero, the presence of oxygen can be recognized because the ORP profile increases toward positive values (Figure 6D), indicating oxidative conditions. Stimulated by

solar irradiance, photosynthesis ensures a reasonable production of oxygen. In this phase, it is pointless to provide external oxygen, whilst it is more advantageous completely to exploit the free-of-charge oxygen provided by photosynthetic organisms (microalgae and cyanobacteria). Despite oxidative condition at the end of this phase, zero-DO values suggest that the oxidation process is not completed, and hence some biodegradable COD and NH_4^+ may still be in the reactor. If nitrification is not completed, nitrite, along with nitrate, may be found.

2) "Zero-DO+dark" phase (progressive time = 16-24 h): this is defined by the beginning of the first dark period (DP1) and zero-DO concentration. In the dark, no oxygen production occurs, and respiration (i.e. oxygen consumption) results in a zero-DO concentration. Figure 6D shows that as soon as the light is turned off, the ORP profile presents an immediate decrease and then remains approximately stable during the whole dark period. In this phase, local anoxic condition may occur. Therefore, if biodegradable COD is available, denitrification of nitrate produced during the "Zero DO+light-phase" may take place. However, since the pH profile does not show a significant trend (Figure 6C), denitrification is a minor process.

3) "Sunrise" phase (progressive time = 24-28 h): this is denoted by a significant increase in the DO concentration that usually occurs during the second light period (LP2) when solar irradiance increases. The DO reaches a peak, in correspondence to the maximum irradiance that occurs around midday. As observed in section 3.2, the DO peak may reach oversaturation level. In this phase, the oxygen production surpasses the oxygen demand of the biomass. Because biodegradable substrates were depleted in the previous phases, only a small residual NH_4^+ concentration may remain and oxygen is mainly consumed by respiration. Indeed, the DO profile shown in Figure 6A is similar to that of Figure 5C (observed when only respiration occurred). Since photosynthetic oxygenation prevails over oxygen consumption, DO

increases sharply (Figure 6A). Also ORP increases significantly towards positive values (Figure 6D), indicating oxidative conditions. In this phase, along with DO, pH increases remarkably due to photosynthesis. This effect was not counterbalanced by the acidification produced by bacterial nitrification due to the scarcity or absence of NH_4^+ that was consumed in the previous phases.

High DO values together with high ORP values (oxidative condition) suggest that the oxidation process is completed. Therefore, biodegradable COD and NH_4^+ have been consumed. Since the nitrification is completed, only nitrate should be found.

4) "Sunset" phase (progressive time = 28-40 h): this is characterized by the decrease of DO together with the decrease of solar irradiance.

As a consequence of the progressive reduction of solar irradiance during the second light period (LP2), photosynthetic activity slows down. Therefore, since endogenous respiration is almost constant while oxygen production diminishes, this results in a decreasing DO profile (Figure 6B). Depending on the balance between produced and consumed oxygen, DO profile may decrease with a more or less steep slope. However, if the production of oxygen equals the oxygen consumed by the biomass, DO profile may remain constant. As shown in figure 6D, high ORP values demonstrates that DO is enough to maintain oxidative conditions. The reduction of photosynthetic activity lead to a less uptake of HCO_3^- (see section 3.3.2) and therefore pH profile decreases progressively (Figure 6C).

5) "Dark" phase (time = 40-48 h): this coincides with the second dark period (DP2).

Due to the absence of photosynthesis in the dark, DO is progressively consumed and, depending on the respiration rate, may reach zero. Since in this phase only respiration occurs, the slope of DO profile can be exploited to calculate the Oxygen Uptake Rate (OUR) of the biomass (Figure 7). Considering the three cycles of Figure 6, an average volumetric OUR of 1.8±0.3 mg O_2 L^{-1} h^{-1} was obtained taking into

account the linear part of the curves (Figure 7). The volumetric OUR obtained corresponds to a specific value of 1.6±0.3 mg O_2 g TSS^{-1} h^{-1} (TSS = 1.18±0.1 g TSS/L). The OUR calculated certainly corresponds to the endogenous respiration of the biomass, because in this final phase of the cycle biodegradable substrates and ammonium can be considered completely oxidized. As shown in figure 6D, ORP decreases as a consequence of oxygen consumption but does not reach low negative values. ORP reaches the minimum values (< -100 mV) during the subsequent feeding of anaerobic fresh wastewater that induces a change from aerobic conditions to a fermentation stage.

Although local anoxic condition may occur inside the flocs, denitrification of the remaining nitrate can be excluded because biodegradable COD is not available.

< insert Figure 7 here >

From the profiles of DO, pH and ORP it was possible to identify some relevant characteristic points (discussed in the following sections). These characteristic points may be exploited in the on-line control and optimization of the process.

3.3.1. "DO breakpoint" and "Ammonia Valley" reveal the end-point of ammonium

No external aeration was provided in the PSBR, and oxygen was produced only during the light periods of the cycle. As observed in section 3.3, bacterial oxidation, in particular nitrification, causes a consumption of DO that may drop to zero (Zero DO+light phase). In regard to nitrification, the utilization of alkalinity leads to a progressive decrease of pH according to the following reaction [27].

$$0.098CO_2 + NH_4^+ + 1.863O_2 + \rightarrow 0.0196\ C_5H_7NO_2 + 0.98NO_3^- + 0.0941\ H_2O + 1.98H^+$$

As shown in figure 6C, pH decreases during the "Zero-DO+light phase" indicating that the acid-based effect by nitrification dominated in the reactor. Once nitrification is

448 complete and ammonium is totally oxidized, DO is no longer consumed for this
449 purpose, and its concentration raises very rapidly and sharply due to the continuous
450 oxygen production by photosynthesis (Sunrise phase, Figure 6B), which depends on the
451 available light. Consequently, also pH increases sharply (Figure 6C).
452 The endpoint of ammonium originates a characteristic point in the DO profile called
453 "DO breakpoint", indicated in the three cycles of Figure 6B. The "DO breakpoint"
454 occurs in concomitance with a characteristic point in the pH profile as shown in Figure
455 6C: when ammonium is completely depleted, pH starts to rise and a local minimum
456 called "Ammonia valley" occurs in the pH profile. The increase in pH could be due to
457 stripping of CO_2 from the system, but She et al. [33] suggested that it might be related
458 to the buffer capacity of the medium after ammonium oxidation is finished.
459 Since TKN load is widely fluctuating in the influent real wastewater, the completion of
460 nitrification may have different durations, so that Ammonia valley may appear in the
461 "Zero-DO+light" phase (see 3rd cycle in Figure 6C) or in the subsequent "Sunrise"
462 phase (see 1st and 2nd cycles in Figure 6C).
463 The perfect correspondence between the endpoint of ammonium and the two
464 characteristic points (DO breakpoint + Ammonia valley) was demonstrated in the track
465 study of Figure 8.
466 Figure 8A shows that as soon as ammonia oxidation is completed, DO and pH rise
467 sharply. Also the ORP profile showed a change in slope (Figure 8B), but this behavior
468 was not always appreciable in all the cycles. Thus, ORP is not recommended for an on-
469 line control of the process. Conversely, the two characteristic points "DO breakpoint"
470 and "Ammonia valley" can be recognized very well and can thus be usefully exploited
471 to identify the conclusion of the cycle when ammonium removal is required. The
472 breakpoint in the DO curve, also named "ammonium breakpoint", coupled with the
473 "ammonia valley" was effectively used by She et al. [33] to indicate the end point of

nitritation and to adjust the duration of the aerobic phase in accordance with the variation of influent NH_4^+-N concentration, avoiding from high DO and excess aeration. In the track study of Figure 8, the ammonium removal rate was 2.04 mg NH_4^+-N L^{-1} h^{-1} (corresponding to 2.57±0.32 mg NH_4^+-N g TSS^{-1} h^{-1}; TSS concentration in the PSBR was 0.79±0.1 g TSS/L). To be noted is that this remarkable nitrification rate was obtained without external aeration (thus without electric energy) and with a DO profile close to zero. Moreover, the specific rate of 2.57±0.32 mg NH_4^+-N g TSS^{-1} h^{-1} was similar to typical ranges expected for activated sludge.

At the same time, nitrates were produced at a rate of 0.71 mg NO_3^--N L^{-1} h^{-1} (corresponding to 0.90±0.12 mg NO_3^--N g TSS^{-1} h^{-1}, approximately half of the nitrification rate), indicating that denitrification occurred due to the low DO in the bulk liquid.

< *insert Figure 8 here* >

3.3.2. At the maximum irradiance, the peaks of DO, pH and ORP reveal the end of the treatment

As shown in section 3.2, the maximum irradiance is associated with the maximum of photosynthetic activity. According to the following reaction [34]:

$$106\ HCO_3^- + 16NH_4^+ + HPO_4^{2-} + 92\ H^+ \rightarrow C_{106}H_{263}O_{110}N_{16}P + 106O_2$$

HCO_3^- uptake dominates the acid-base effect of photosynthesis. Therefore, during the light periods a pH increase is induced in the system so that HCO_3^- uptake may result in a peak of pH at maximum irradiance.

In regard to photosynthetic oxygenation, at maximum irradiance, oxygen consumption affects the extent of the DO peak. The relative maximum in the ORP profile appears in correspondence to the peak of irradiance due to aerobic conditions stimulated by a higher rate of photosynthesis.

The coincidence between the maximum irradiance and the absolute peaks of DO, pH and ORP can be appreciated in the "Sunrise" phase of Figure 6.

During the "Zero-DO+light" phase, there is a large amount of biodegradable substrate to be oxidized. Therefore, due to high oxygen consumption the peaks of DO is very small and in some cases it may be difficult to recognize (Figure 6B). In this phase, nitrification counterbalances the acid-base effect of photosynthesis, affecting the extent of pH peak (Figure 6C). Moreover, a less marked ORP peak (Figure 6D) is the result of the feed of anaerobic fresh wastewater which induces anoxic conditions and thus negative ORP values at the beginning of the cycle.

In the subsequent "Sunrise" phase, when the irradiance is maximum, the peaks of DO, pH and ORP become more sharply defined and reach higher values, because the biodegradable substrates are completely removed.

To sum up, the achievement of well-defined absolute peaks of DO, pH and ORP is the signal that the wastewater treatment is completed and consequently that the cycle can be concluded. Considering the cycles in Figure 6, control over the process on the basis of these characteristic points permits conclusion of the treatment after 15-26 hours instead of 48 hours, reducing the HRT by more than 45%.

4. CONCLUSIONS

This paper has demonstrated that is possible to exploit continuous measurement of the on-line parameters DO, pH and ORP to evaluate correctly the conclusion of the wastewater treatment and thus shorten the HRT of a PSBR. Although photosynthetic oxygenation strongly affects DO, pH and ORP, characteristic points revealing the state of the ongoing biological process were detected along these complex profiles:

- "Ammonia valley" (pH profile) and "DO breakpoint" (DO profile) as key indicators of the complete ammonium removal;
- Absolute peaks of DO, pH and ORP in conjunction with maximum irradiance, as

detectors of COD and TKN complete removal, indicating that the PSBR cycle could be ended.

In this way, the PSBR cycle was shortened by more than 45%, resulting in a significant reduction of foot-print and costs of the treatment.

ACKNOWLEDGEMENTS

The research reported in this paper did not receive any specific grant from funding agencies in the public, commercial, or not-for-profit sectors.

The authors thanks Giovanna Flaim (Fondazione Edmund Mach, Italy) for her assistance in the investigation of microalgae in the photobioreactor and Andrea Pacini for his help during the experimental work.

REFERENCES

[1] H.F. Ludwig, W.J. Oswald, H.B. Gotaas, V. Lynch, Algal symbiosis in oxidation ponds. 1. Growth characteristics of Euglena gracilis cultured in sewage. Sewage and Industrial Wastes, 23 (1951) 1337-1354.

[2] R. Muñoz, B. Guieysse, Algal-bacterial processes for the treatment of hazardous contaminants: a review, Water Research 40 (2006) 2799–815. doi:10.1016/j.watres.2006.06.011

[3] Y. Su, A. Mennerich, B. Urban, Municipal wastewater treatment and biomass accumulation with a wastewater-born and settleable algal-bacterial culture, Water Research 45 (2011) 3351-3358. doi:10.1016/j.watres.2011.03.046

553 [4] J.S. Arcila, G. Buitrón, Microalgae–bacteria aggregates: effect of the hydraulic
554 retention time on the municipal wastewater treatment, biomass settleability and
555 methane potential, Journal of Chemical Technology and Biotechnology (2016).
556 http://dx.doi.org/10.1002/jctb.4901
557 [5] Y. Wang, S. Ho, C. Cheng, W. Guo, D. Nagarajan, N. Ren, D. Lee, J. Chang,
558 Perspectives on the feasibility of using microalgae for industrial wastewater
559 treatment, Bioresource Technology 222 (2016) 485-497.
560 http://dx.doi.org/10.1016/j.biortech.2016.09.106
561 [6] A.L. Gonçalves, J.C.M. Pires, M. Simões, A review on the use of microalgal
562 consortia for wastewater treatment, Algal Research 24 (2017) 403-415.
563 http://dx.doi.org/10.1016/j.algal.2016.11.008
564 [7] N.G.A.I. Karya, N.P. van der Steen, P.N.L. Lens, Photo-oxygenation to support
565 nitrification in an algal–bacterial consortium treating artificial wastewater,
566 Bioresource Technology 134 (2013) 244-250.
567 http://dx.doi.org/10.1016/j.biortech.2013.02.005
568 [8] G. Mujtaba, M. Rizwan, K. Lee, Removal of nutrients and COD from wastewater
569 using symbiotic co-culture of bacterium Pseudomonas putida and immobilized
570 microalga *Chlorella vulgaris*, Journal of Industrial and Engineering Chemistry 49
571 (2017) 145-151. http://dx.doi.org/10.1016/j.jiec.2017.01.021
572 [9] C. Alcántara, J.M. Domínguez, D. García, S. Blanco, R. Pérez, P.A. García-Encina,
573 R. Muñoz, Evaluation of wastewater treatment in a novel anoxic–aerobic algal–
574 bacterial photobioreactor with biomass recycling through carbon and nitrogen mass
575 balances, Bioresource Technology 191 (2015) 173-186.
576 http://dx.doi.org/10.1016/j.biortech.2015.04.125
577 [10] G. Mujtaba, K. Lee, Treatment of real wastewater using co-culture of immobilized
578 Chlorella vulgaris and suspended activated sludge, Water Research 120 (2017) 174-

184. http://dx.doi.org/10.1016/j.watres.2017.04.078

[11] S. Van Den Hende, E. Carré, E. Cocaud, V. Beelen, N. Boon, H. Vervaeren, Treatment of industrial wastewaters by microalgal bacterial flocs in sequencing batch reactors, Bioresource Technology 161 (2014) 246-254. http://dx.doi.org/10.1016/j.biortech.2014.03.057

[12] D. García, C. Alcántara, S. Blanco, R. Pérez, S. Bolado, R. Muñoz, Enhanced carbon, nitrogen and phosphorus removal from domestic wastewater in a novel anoxic-aerobic photobioreactor coupled with biogas upgrading, Chemical Engineering Journal 313 (2017) 424-434. http://dx.doi.org/10.1016/j.cej.2016.12.054

[13] S.J. Judd, L.J.P. van den Broeke, M. Shurair, Y. Kuti, H. Znad, Algal remediation of CO2 and nutrient discharges: a review, Water Research 87 (2015) 356-366. http://dx.doi.org/10.1016/j.watres.2015.08.021

[14] D.L. Sutherland, M.H. Turnbull, P.A. Broady, R.J. Craggs, Effects of two different nutrient loads on microalgal production, nutrient removal and photosynthetic efficiency in pilot-scale wastewater high rate algal ponds, Water Res. 66 (2014) 53-62.

[15] Y.Z. Peng, Y. Maa, S.Y. Wang, Improving nitrogen removal using on-line sensors in the A/O process, Biochemical Engineering Journal 31 (2006) 48–55. doi:10.1016/j.bej.2006.05.023

[16] G. Olsson, M.K. Nielsen, A.L. Jensen, Z. Yuan, Instrumentation, Control and Automation in Wastewater Systems. Scientific and Technical Report No. 15. IWA Publishing, London, 2005.

[17] E. Paul, S. Plisson-Saune, M. Mauret, J. Cantet, Process state evaluation of alternating oxic-anoxic activated sludge using ORP, pH and DO, Water Science and Technology 38 (1998) 299-306.

[18] P. Tanwar, T. Nandy, P. Ukey, P. Manekar, Correlating on-line monitoring

parameters, pH, DO and ORP with nutrient removal in an intermittent cyclic process bioreactor system, Bioresource Technology 99 (2008) 7630-7635. doi:10.1016/j.biortech.2008.02.004

[19] P.T. Martín de la Vega, E. Martínez de Salazar, M.A. Jaramillo, J. Cros, New contributions to the ORP & DO time profile characterization to improve biological nutrient removal, Bioresource Technology 114 (2012) 160-167. http://dx.doi.org/10.1016/j.biortech.2012.03.039

[20] G. Andreottola, P. Foladori, M. Ragazzi, On-line control of a SBR system for nitrogen removal from industrial wastewater, Water Science and Technology, 43 (2001) 93–100.

[21] H. Kim, O.J. Hao, pH and oxidation-reduction potential control strategy for optimization of nitrogen removal in an alternating aerobic-anoxic system, Water Environ Res. 73 (2001) 95-102.

[22] L. Zanetti, N. Frison, E. Nota, M. Tomizioli, D. Bolzonella, F. Fatone, Progress in real-time control applied to biological nitrogen removal from wastewater. A short-review, Desalination 286 (2012) 1-7. doi:10.1016/j.desal.2011.11.056

[23] W. Zhao, Y. Zhang, D. Lv, M. Wang, Y. Peng, B. Li, Advanced nitrogen and phosphorus removal in the pre-denitrification anaerobic/anoxic/aerobic nitrification sequence batch reactor (pre-A2NSBR) treating low carbon/nitrogen (C/N) wastewater, Chemical Engineering Journal 302 (2016) 296–304.

[24] O. Tiron, C. Bumbac, I.V. Patroescu, V.R. Badescu, C. Postolache, Granular activated algae for wastewater treatment, Water Science and Technology 71 (2015), 832-839. doi:10.2166/wst.2015.010

[25] M. Wang, H. Yang, S.J. Ergas, P. van der Steen, A novel shortcut nitrogen removal process using an algal-bacterial consortium in a photo-sequencing batch reactor (PSBR), Water Research 87 (2015) 38-48.

631 http://dx.doi.org/10.1016/j.watres.2015.09.016
632 [26] APHA, AWWA, WEF, Standard Methods for the Examination of Water and
633 Wastewater, 22 ed. American Public Health Association, Washington, D.C. 2012.
634 [27] G. Tchobanoglous, F.L. Burton, H.D. Stensel, Wastewater engineering: treatment
635 and reuse. 4th ed., McGraw-Hill Metcalf & Eddy Inc., Boston. 2003
636 [28] E. Posadas, M. del Mar Morales, C. Gomez, F.G. Acién, R. Muñoz, Influence of
637 pH and CO2 source on the performance of microalgae-based secondary domestic
638 wastewater treatment in outdoors pilot raceways, Chemical Engineering Journal 265
639 (2015) 239-248. doi: 10.1016/j.cej.2014.12.059.
640 [29] L. Christenson, R. Sims, Production and harvesting of microalgae for wastewater
641 treatment, biofuels, and bioproducts, Biotechnology Advances 29 (2011) 686–702.
642 doi:10.1016/j.biotechadv.2011.05.015
643 [30] J.B.K. Park, R.J. Craggs, A.N. Shilton, Recycling algae to improve species control
644 and harvest efficiency from a high rate algal pond. Water Research 45 (2011) 6637-
645 6649. doi:10.1016/j.watres.2011.09.042
646 [31] B. Zhang, P.N.L. Lens, W. Shi, R. Zhang, Z. Zhang, Y.Guo, X. Bao, F. Cui,
647 Enhancement of aerobic granulation and nutrient removal by an algal–bacterial
648 consortium in a lab-scale photobioreactor, Chemical Engineering Journal 334 (2018)
649 2373–2382.
650 [32] J. Yang, Y. Gou, F. Fang, J. Guo, L. Lu, Y. Zhou, H. Ma, Potential of wastewater
651 treatment using a concentrated and suspended algal-bacterial consortium in a photo
652 membrane bioreactor, Chemical Engineering Journal 335 (2018) 154–160.
653 [33] Z. She, L. Zhao, X, Zhang, C. Jin, L. Guo, S. Yang, Y. Zhao, M. Gao, Partial
654 nitrification and denitrification in a sequencing batch reactor treating high-salinity
655 wastewater, Chemical Engineering Journal 288 (2016) 207–215
656 [34] F.M.M. Morel, J.G. Hering, Principles and Applications of Aquatic Chemistry,

John Wiley & Sons Inc, New York. 1993.

660 **CAPTIONS OF FIGURES**

661 *Figure 1. (A) The photo-sequencing batch reactor. (B) Microscopic observations of*
662 *microalgae-bacteria clusters. (C) Very good settleability of the biomass in the Imhoff*
663 *cone.*

664

665 *Figure 2. Sequence of the light and dark periods, and overview of the ongoing-*
666 *biological process in the PSBR typical cycle.*

667

668 *Figure 3. (A) COD and sCOD in the influent and effluent wastewater and removal*
669 *efficiency of COD; (B) TKN and NH4+-N in the influent and effluent wastewater and*
670 *removal efficiency of TKN.*

671

672 *Figure 4. (A) Profiles of COD, NH_4-N, NO_2-N and NO_3-N during light and dark phases*
673 *in an entire 48-hour typical cycle. (B) Profiles of online parameters pH and DO.*

674

675 *Figure 5. Irradiance and DO profiles during the PSBR cycle (without feeding) with*
676 *different light sources: (A) sunlight; (B) artificial light; (C) sunlight + artificial light.*

677

678 *Figure 6. Sequence of three typical cycles in the PSBR and profiles of irradiance, DO,*
679 *pH, ORP. The profiles reveal a sequence of typical phases affected by the alternation of*
680 *light and dark periods, and related to the treatment process.*

681

682 *Figure 7. Endogenous Oxygen Upake Rate of the biomass obtained from the profile of*
683 *DO concentration during the "Dark" phase.*

684

685 *Figure 8. Track study in the PSBR to demonstrate the coincidence of two characteristic*

686 *points (DO breakpoint + Ammonia valley) and the endpoint of ammonium.*

687

688

689 **CAPTIONS OF TABLES**

690 *Table 1. Characterization of influent and effluent wastewater and removal efficiency in*

691 *the PSBR (avg.±st.dev.).*

692

Table 1

Parameter	No. samples in influent and effluent	Concentration (mg/L)		Removal efficiency (%)
		Influent	Effluent	
COD	16-45	292±101	34±9	87±5
sCOD	16-45	119±21	25±9	79±3
TKN	16-45	64±20	1.2±1.2	98±2
NH_4^+-N	16-45	55±13	0.6±1.2	99±3
NO_2^--N	16-45	0.1±0.1	0.1±0.1	-
NO_3^--N	16-45	1.1±0.3	19.0±7.4	-
Total N	16-45	66±20	20±7	68±10
PO_4^{3-}-P	16-45	2.7±0.8	2.2±0.8	16±17
TSS	16-13	143±72	7.4±6.3	93±4

Figure 1

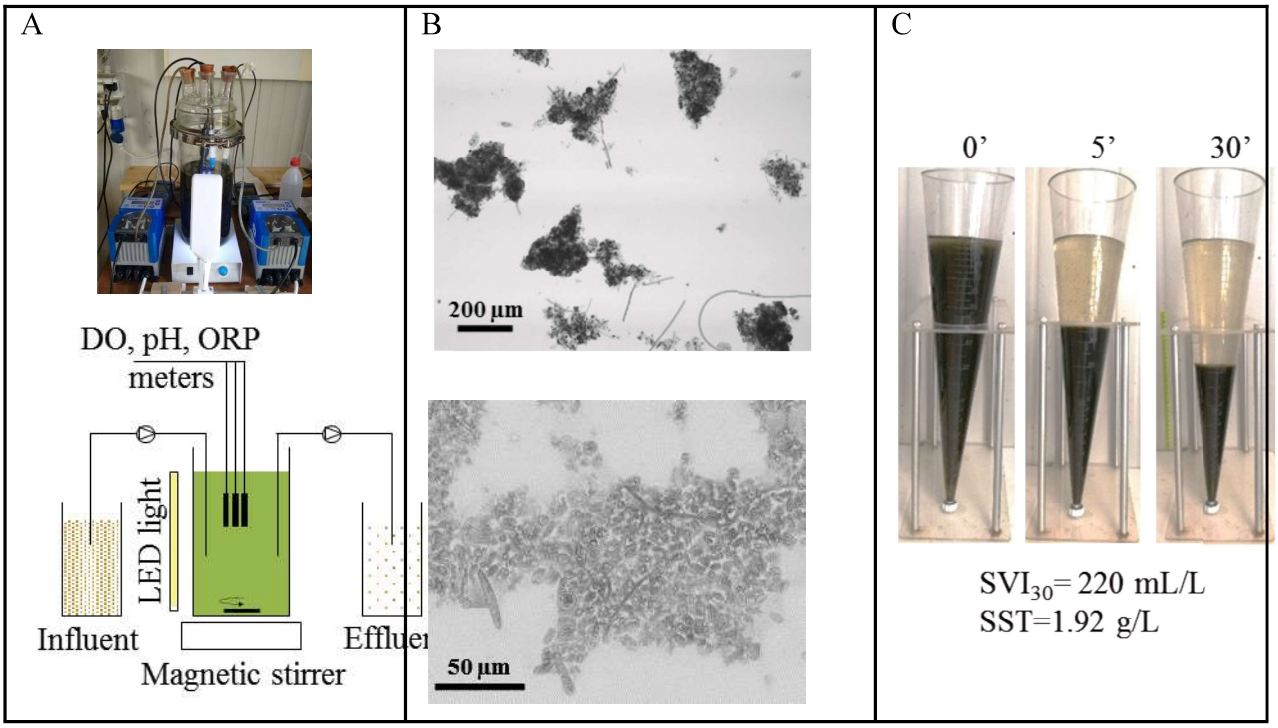
A
DO, pH, ORP
meters
LED light
Influent
Effluent
Magnetic stirrer
B
200 µm
50 µm
C
0'
5'
30'
SVI30= 220 mL/L
SST=1.92 g/L

Figure 2

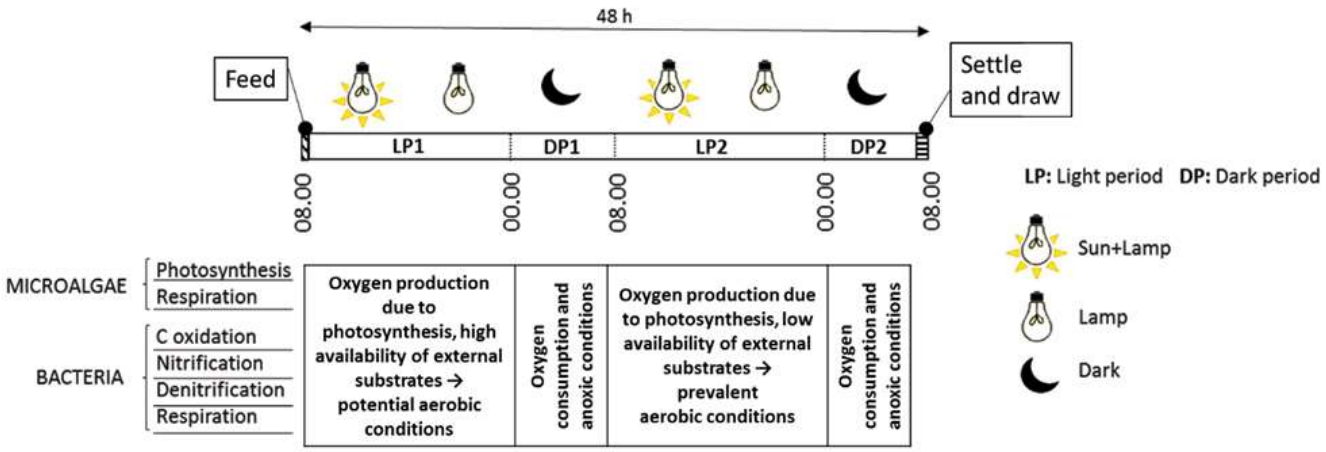
48 h
Feed
Settle and draw
LP1
DP1
LP2
DP2
08.00
00.00
08.00
00.00
08.00
LP: Light period
DP: Dark period
Sun+Lamp
Lamp
Dark
MICROALGAE
Photosynthesis
Respiration
BACTERIA
C oxidation
Nitrification
Denitrification
Respiration
Oxygen production due to photosynthesis, high availability of external substrates → potential aerobic conditions
Oxygen consumption and anoxic conditions
Oxygen production due to photosynthesis, low availability of external substrates → prevalent aerobic conditions
Oxygen consumption and anoxic conditions

Figure 3

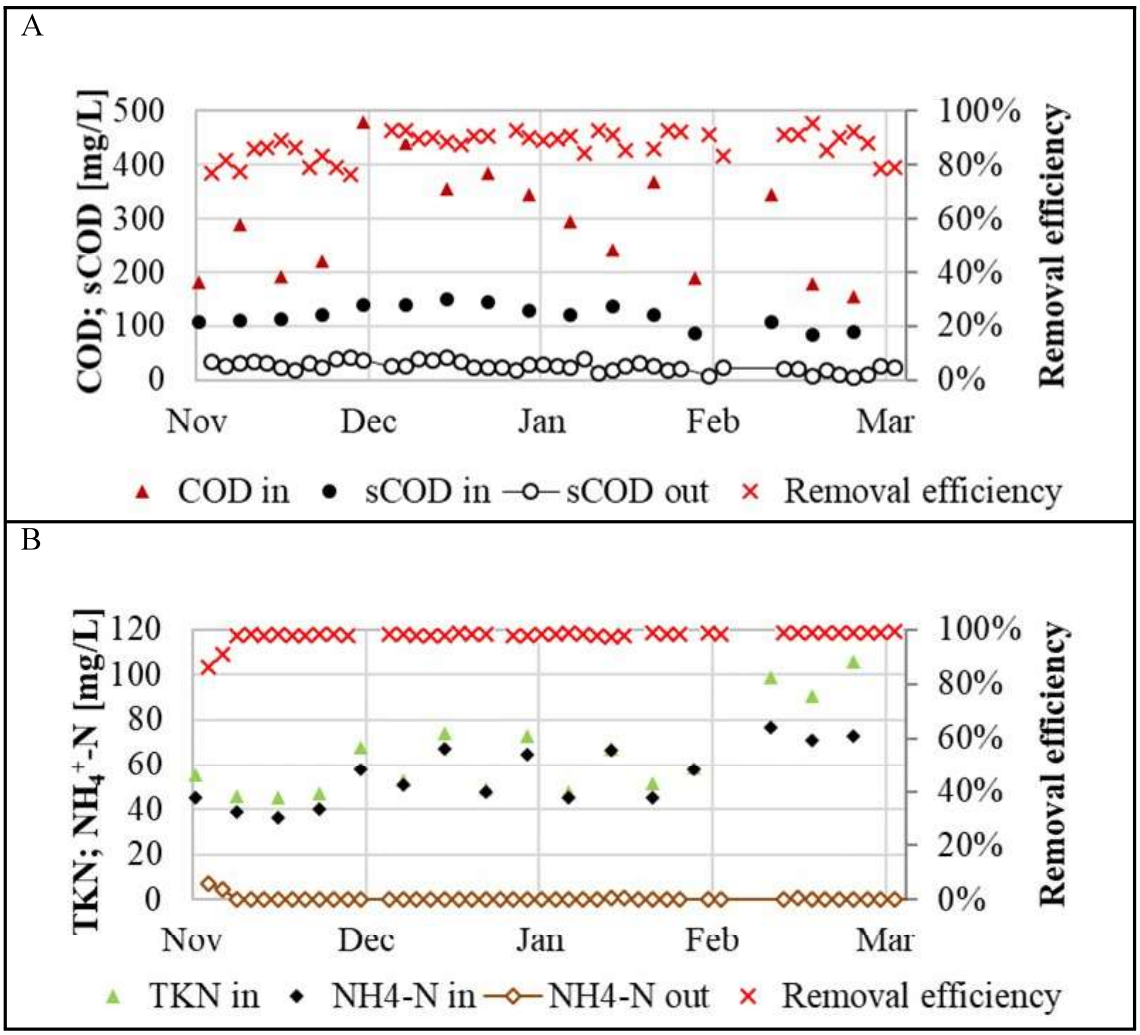
A
COD; sCOD [mg/L]
500
400
300
200
100
0
100%
80%
60%
40%
20%
0%
Removal efficiency
Nov
Dec
Jan
Feb
Mar
COD in
sCOD in
sCOD out
Removal efficiency
B
TKN; NH4+-N [mg/L]
120
100
80
60
40
20
0
100%
80%
60%
40%
20%
0%
Removal efficiency
Nov
Dec
Jan
Feb
Mar
TKN in
NH4-N in
NH4-N out
Removal efficiency

Figure 4

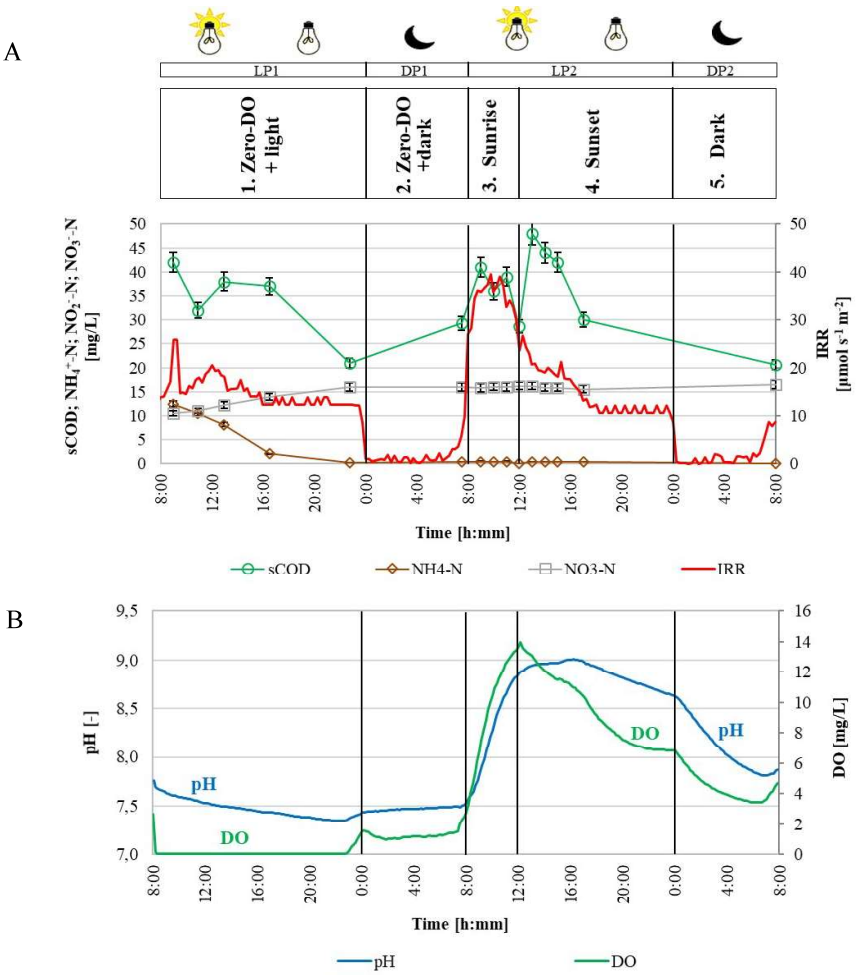
A
LP1
DP1
LP2
DP2
1. Zero-DO + light
2. Zero-DO +dark
3. Sunrise
4. Sunset
5. Dark
sCOD; NH4+-N; NO2-N; NO3-N [mg/L]
IRR [µmol s-1 m-2]
Time [h:mm]
sCOD
NH4-N
NO3-N
IRR
B
pH [-]
DO [mg/L]
pH
DO
Time [h:mm]
pH
DO

Figure 5

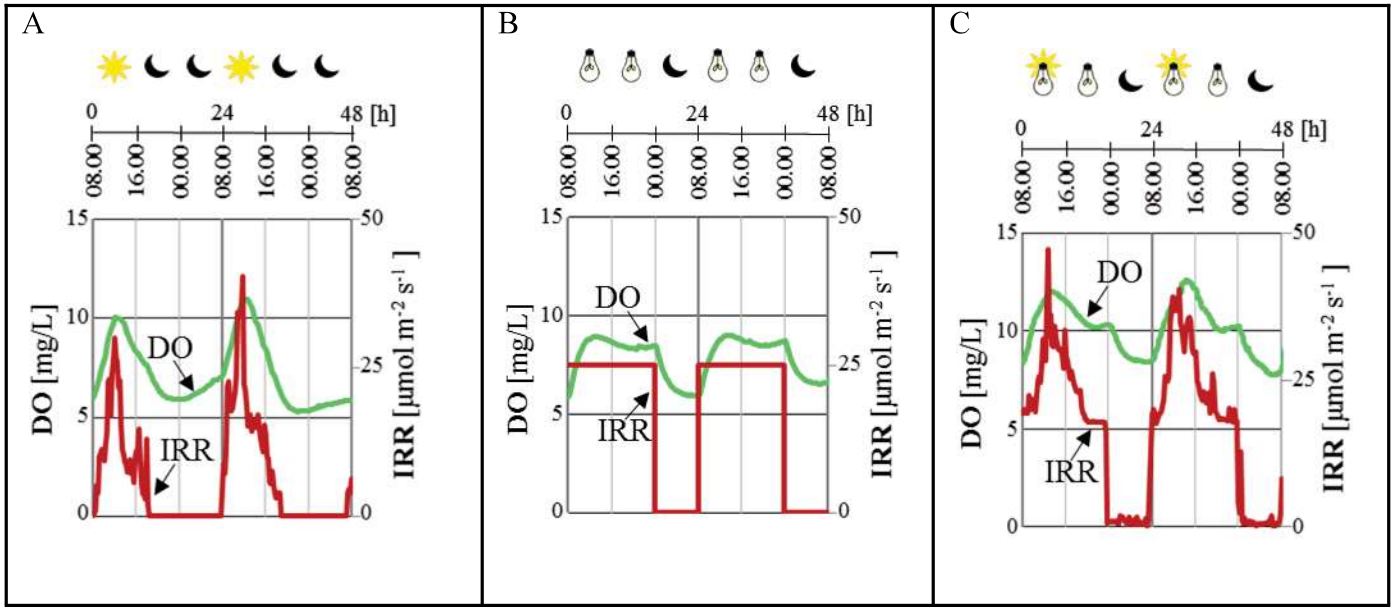
A
B
C
0
24
48 [h]
08.00
16.00
00.00
08.00
16.00
00.00
08.00
15
10
5
0
50
25
0
DO [mg/L]
IRR [µmol m-2 s-1]
DO
IRR

Figure 6

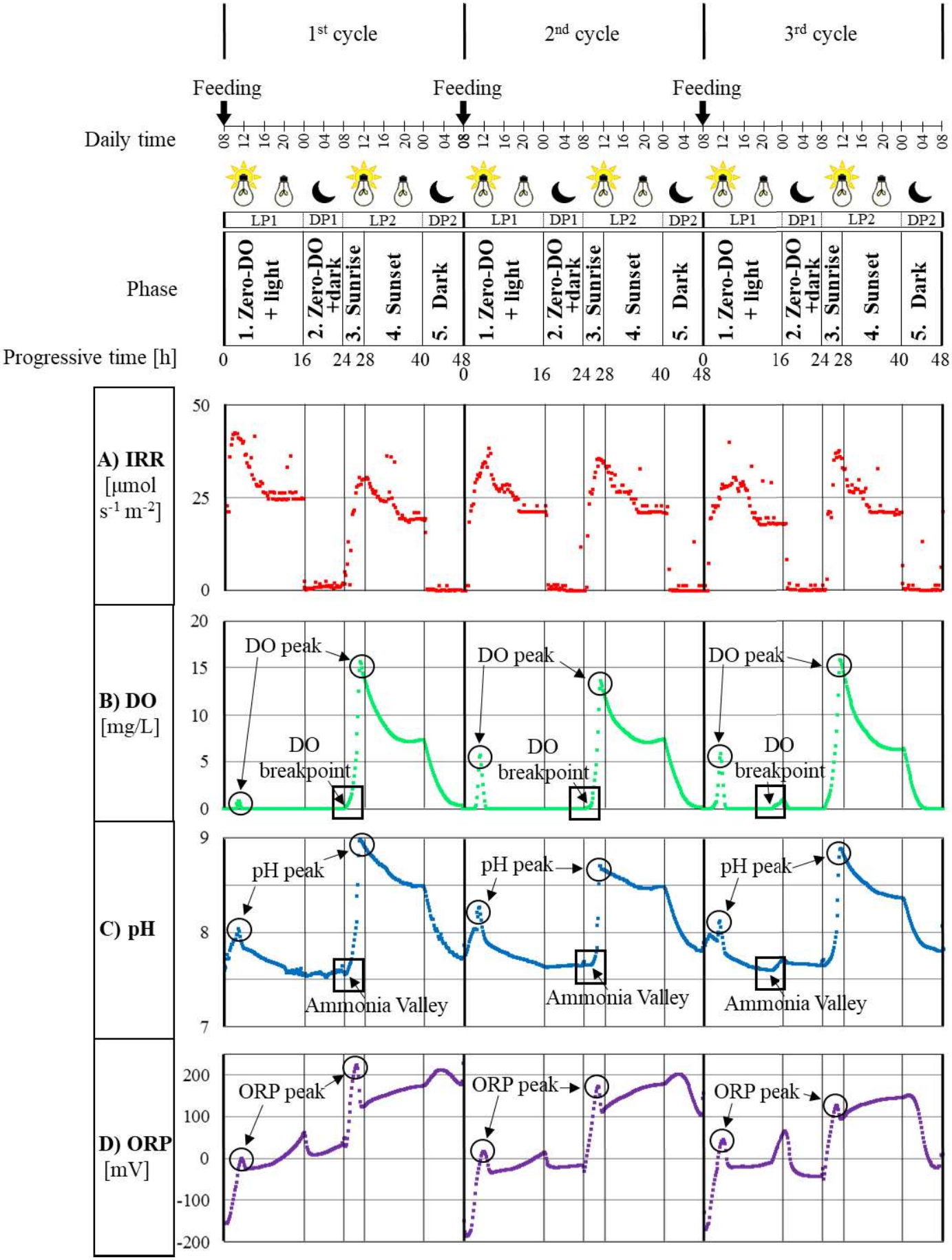
1st cycle
2nd cycle
3rd cycle
Feeding
Feeding
Feeding
Daily time
LP1
DP1
LP2
DP2
Phase
1. Zero-DO + light
2. Zero-DO +dark
3. Sunrise
4. Sunset
5. Dark
Progressive time [h]
A) IRR [µmol s-1 m-2]
B) DO [mg/L]
DO peak
DO breakpoint
C) pH
pH peak
Ammonia Valley
D) ORP [mV]
ORP peak

Figure 7

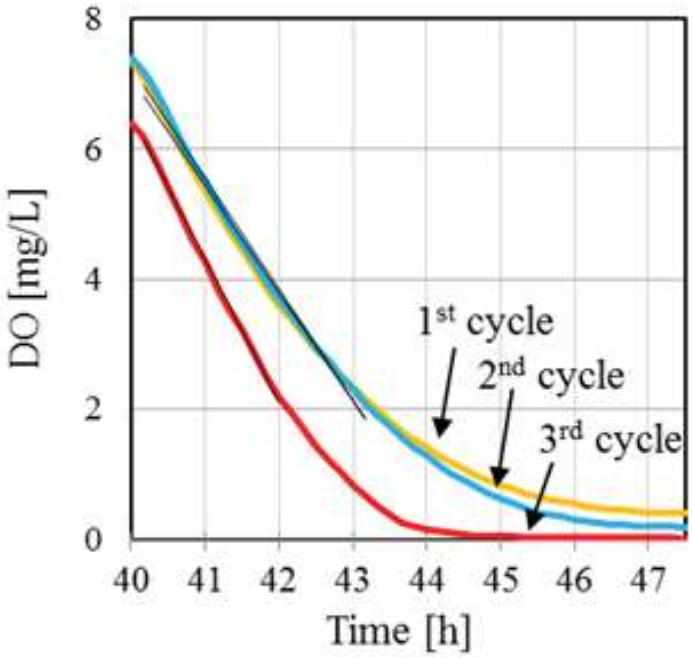
8
6
4
2
0
DO [mg/L]
40
41
42
43
44
45
46
47
Time [h]
1st cycle
2nd cycle
3rd cycle

Figure 8

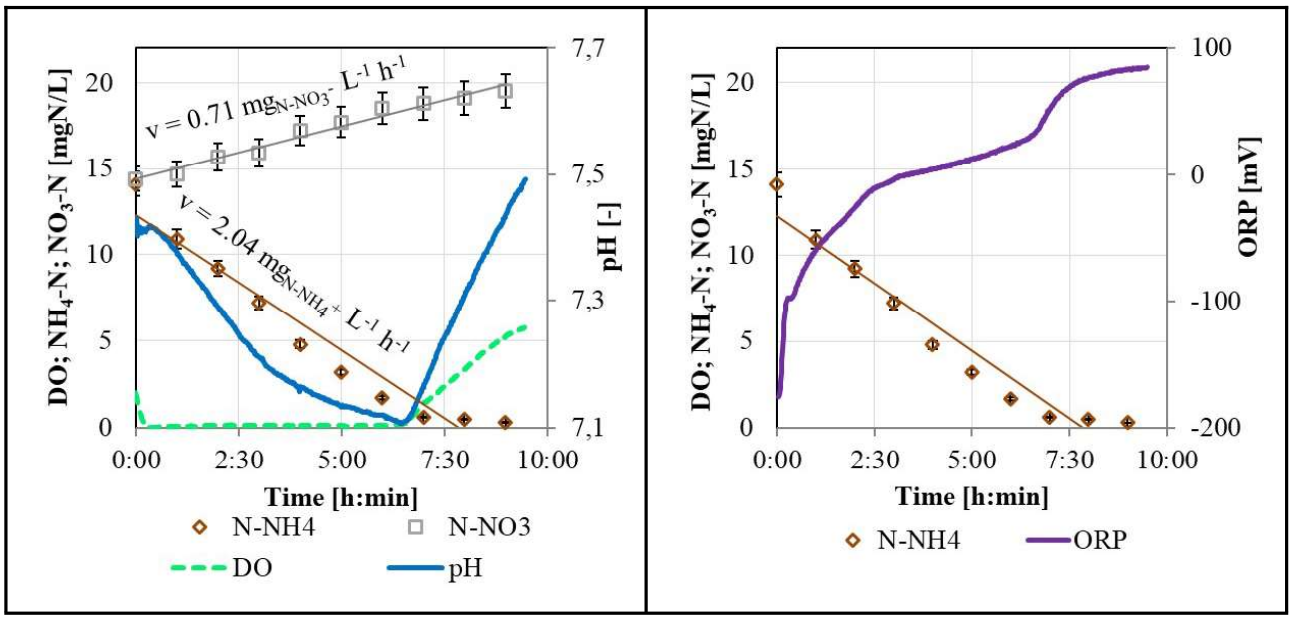
DO; NH4-N; NO3-N [mgN/L]
pH [-]
v = 0.71 mgN-NO3- L-1 h-1
v = 2.04 mgN-NH4+ L-1 h-1
Time [h:min]
N-NH4
N-NO3
DO
pH
ORP [mV]
ORP